

Comparing biofilm models for a single species biofilm system

E. Morgenroth*, H.J. Eberl**, M.C.M. van Loosdrecht***, D.R. Noguera****, G.E. Pizarro****,*****, C. Picioreanu***, B.E. Rittmann*****, A.O. Schwarz***** and O. Wanner*****

* Department of Civil and Environmental Engineering and Department of Animal Sciences, University of Illinois at Urbana-Champaign, 205 N. Mathew Ave., Urbana, IL 61801, USA (E-mail: emorgenr@uiuc.edu)

** Department of Mathematics and Statistics, University of Guelph, Guelph, ON, N1G 2W1, Canada

*** Kluyver Institute for Biotechnology, Technical University of Delft, Julianalaan 67, 2628 BC Delft, The Netherlands

**** Department of Civil and Environmental Engineering, University of Wisconsin, Madison, WI, USA

***** Department of Hydraulics and Environmental Engineering, Pontificia Universidad Católica de Chile, Santiago, Chile

***** Department of Civil Engineering, Northwestern University, 2145 Sheridan Road, Evanston, IL 60208-3109, USA

***** Urban Water Management Department, Swiss Federal Institute of Environmental Science and Technology (EAWAG), CH-8600 Dübendorf, Switzerland

Abstract A benchmark problem was defined to evaluate the performance of different mathematical biofilm models. The biofilm consisted of heterotrophic bacteria degrading organic substrate and oxygen. Mathematical models tested ranged from simple analytical to multidimensional numerical models. For simple and more or less flat biofilms it was shown that analytical biofilm models provide very similar results compared to more complex numerical solutions. When considering a heterogeneous biofilm morphology it was shown that the effect of an increased external mass transfer resistance was much more significant compared to the effect of an increased surface area inside the biofilm.

Keywords Benchmark problem; biofilm model; biofilm morphology; mass transfer

Introduction

New experimental and mathematical modeling techniques have over recent years improved our understanding of the significance of the spatial structure of biofilms. As a result, an increasing number of multidimensional mathematical models have been developed. In this situation both researchers and practitioners often have difficulties in selecting appropriate models for their application (Morgenroth *et al.*, 2000b). An IWA Task Group on Biofilm Modeling was established to evaluate the merit of these different modeling approaches ranging from simple analytical to complex numerical models using a series of benchmark problems for a side-by-side comparison (Noguera and Morgenroth, 2004).

In this first benchmark problem (BM1) a simple biofilm system is defined with one particulate compound (active heterotrophic biomass) and two soluble compounds (organic substrate and oxygen). The overall purpose of BM1 was to create a baseline comparison of the different modeling approaches in a system that was equally suited for all modeling approaches. Based on BM1, further benchmark problems were defined to evaluate the influence of hydrodynamics in a heterogeneous biofilm (BM2, Eberl *et al.*, 2004) and to evaluate competition between different types of biomass (BM3, Rittmann *et al.*, 2004). The specific objectives of BM1 were to define a list of performance indices that could subsequently be used to compare the different modeling approaches. These performance indices should include both biofilm related parameters (e.g., substrate flux) and an evaluation of

the user friendliness of different modeling approaches. Based on comparisons within BM1, recommendations for researchers and practitioners on the selection of an appropriate model for a simple system such as the one used in BM1 are being made.

System definition

BM1 described a simple biofilm system on a flat substratum in contact with a completely mixed bulk phase. The standard parameters describing the physical system are summarized in Table 1. For the organic substrate the influent concentration was given while for the electron acceptor the bulk phase concentration above the biofilm was fixed (e.g., through aeration). A single biological growth process was defined where heterotrophic biomass in the biofilm grew using an organic substrate as the electron donor and oxygen as the electron acceptor (Table 2, Table 3). No conversion processes were assumed to take place in the bulk phase. A lysis process was defined that reduced the amount of active biomass. Only one particulate component was considered (X_H = active biomass) and lysis was assumed not to produce any particulate products. Thus, the resulting biofilm by definition had a constant biomass density over the thickness of the biofilm. The lysis process influenced modeling results only if lysis was larger than the amount of active biomass produced in the growth process resulting in a reduced biofilm thickness. In this case the biofilm thickness was found from a balance between growth and lysis. If growth of active biomass exceeded lysis then the specified average biofilm thickness was maintained by detachment.

In BM1 five cases as defined in Table 4 were evaluated using different modeling approaches. These cases were defined to evaluate the biofilm under conditions where either the amount of biomass or mass transport were limiting overall performance.

Performance indices

Modeling results were compared using the following performance indices:

Average fluxes and effluent substrate concentrations

Substrate flux (J_S , $M L^{-2} T^{-1}$) determines the overall substrate removal in a biofilm system and under steady state conditions is directly related to the effluent substrate concentration:

Table 1 Standard physical parameters for BM1

Physical parameter	Symbol	Value with units
Flow rate	Q	$0.02 \text{ m}^3/\text{d}$
Reactor volume	V_R	$1.25 \times 10^{-3} \text{ m}^3$
Biofilm surface area	A_f	0.1 m^2
Average biofilm thickness*	L_F	$500 \text{ }\mu\text{m}$
Boundary-layer thickness	L_L	0
Maximum biomass density	$X_{F,Tot} = M_X/V_F$	$1 \times 10^4 \text{ g}_{\text{CODX}}/\text{m}^3$
Substrate (COD) influent concentration	$C_{S,in}$	$30 \text{ g}_{\text{CODS}}/\text{m}^3$
Oxygen concentration in the bulk water	C_{O_2}	$10 \text{ g}_{\text{O}_2}/\text{m}^3$

* This average biofilm thickness results from a total biomass of $0.5 \text{ g}_{\text{COD}}$ and the given biofilm surface area and density

Table 2 Matrix of stoichiometry and kinetic expressions used for BM1

	X_H	C_S	C_{O_2}	Rate [$M L^{-3} T^{-1}$]
Heterotrophic growth	1	$-1/Y_H$	$-(1-Y_H)/Y_H$	$\mu_H \frac{C_S}{K_S + C_S} \cdot \frac{C_{O_2}}{K_{O_2} + C_{O_2}} X_H$
Heterotrophic lysis	-1			$k_H \cdot X_H$

Table 3 Kinetic and stoichiometric parameters for BM1

Parameter	Symbol	Value with Units
Maximum specific utilization rate	μ_{\max}	6 d ⁻¹
Lysis rate	k_H	0.4 d ⁻¹
Substrate half-maximum-rate concentration	K_S	4 g _{CODS} /m ³
Oxygen half-maximum-rate concentration	K_{O_2}	0.2 g _{O₂} /m ³
True yield	Y_H	0.63 g _{CODX} /g _{CODS}
Diffusion coefficient in pure water	D_S	1 × 10 ⁻⁴ m ² /d
Diffusion coefficient of O ₂ in pure water	D_{O_2}	2 × 10 ⁻⁴ m ² /d
Ratio of diffusion coefficients in biofilm versus water	$D_{S,F}/D_S$ or $D_{O_2,F}/D_{O_2}$	1

Table 4 Summary of the standard and four special cases used with BM1

#	Case name	Condition	Purpose
1	Standard situation	See Table 1–Table 3	
2	O ₂ limitation	Bulk oxygen concentration: $C_{O_2} = 0.2 \text{ g}_{O_2}/\text{m}^3$	To evaluate how models describe a change of the limiting substrate (oxygen as opposed to organic substrate).
3	Biomass limitation	Average biofilm thickness: $L_F = 20 \text{ }\mu\text{m}$	To evaluate how models describe a fully penetrated biofilm.
4	Reduced diffusivity in the biofilm	Biofilm diffusivity/pure water diffusivity: $D_F/D = 0.2$	To evaluate how modeling results are influenced by a change of the <i>internal</i> mass transfer resistance.
5	Mass transfer resistance in the bulk	Concentration boundary layer: $L_L = 500 \text{ }\mu\text{m}$	To evaluate how modeling results are influenced by a change of the <i>external</i> mass transfer resistance.

$$0 = Q \cdot (C_{S,\text{in}} - C_{S,\text{bulk}}) - J_S \cdot A_f \quad (1)$$

where A_f is the area of the biofilm substratum. Note that for heterogeneous biofilm morphologies the interface between biofilm and water is larger than A_f . Fluxes and effluent substrate concentrations are reported for both the organic substrate (C_S) and oxygen (C_{O_2}).

Average biofilm surface concentrations

A comparison of the average concentrations at the surface of the biofilm with bulk phase concentrations is used to discuss the significance of an external mass transfer resistance. The external mass transfer resistance is related to bulk phase and surface concentration as follows:

$$J_S = \frac{C_{S,\text{bulk}} - C_{S,\text{surface}}}{\kappa} \quad (2)$$

where $\kappa = L_L/D_L$ is the external mass transfer resistance, D_L is the diffusion coefficient in the diffusion boundary layer, and L_L is the thickness of the diffusion boundary layer.

Average biofilm base concentration

A comparison of the average concentrations at the base of the biofilm with average concentrations at the surface of the biofilm is used to discuss the significance of internal mass transfer resistances and to evaluate penetration of the biofilm.

User friendliness

In addition to comparing quantitative modeling results the user friendliness is evaluated

based on the availability of software, computational time and memory required, flexibility of the model and availability of parameters.

Applied models

The benchmark was used to compare different modeling approaches ranging from simple analytical models, to standard software for one-dimensional biofilms, to custom-made software for multi-dimensional biofilms. An overview of applied models is presented in Table 5. The first group of biofilm models provided solutions for a flat biofilm morphology. The analytical solution (1D-A) and the pseudo-analytical solution (1D-PA) evaluated only the limiting compound and calculated the non-limiting compound based on overall stoichiometry. Numerical 1-D simulations (1D-N) were performed using a range of approaches. Simple 1-D numerical simulations were done using AQUASIM (Wanner and Reichert, 1996; Wanner and Morgenroth, 2004). The approaches based on Pizarro *et al.* (2001) and Eberl *et al.* (2000) used multidimensional algorithms where the biofilm was restricted to a flat surface morphology and therefore degenerated to a 1-D solution. The simulations using AQUASIM and based on Eberl *et al.* (2000) took into account dual Monod kinetics for organic substrate and oxygen while the simulations based on Pizarro *et al.* (2001) were evaluating the limiting compound only.

The second group of biofilm models took into account effects related to a heterogeneous biofilm morphology while maintaining the same average biofilm thickness as defined in Table 1. The first approach used a true 3-D simulation based on Picioreanu *et al.* (1998) (3D-N). Two different cases were evaluated for 3D-N with different assumptions for the boundary layer thickness. In 3D-N(a) it was assumed that the bulk water above the maximum biofilm thickness was completely mixed while the pore water below the maximum biofilm thickness was stagnant (Figure 1A). For 3D-N(b) it was assumed that the entire water phase (including the pore water) was completely mixed (Figure 1B). A fixed biofilm morphology was used for these 3-D simulations (Figure 2).

A simplified approach to take into account effects of a heterogeneous biofilm morphology is based on the combination of multiple 1-D simulations (Morgenroth and Wilderer, 2000; Morgenroth *et al.*, 2000a). The basic idea for these pseudo multidimensional simulations (P2D-N) is the assumption that even in heterogeneous biofilm morphologies, local mass transport is still mainly perpendicular to the substratum. Thus, in P2D-N local mass transport is simulated one-dimensionally (i.e., based on 1D-N simulations) where the individual 1-D simulations are connected by the assumption that the bulk phase concentration has to be identical for all simulations. The overall system performance is then evaluated based on a linear combination of individual simulations (for details see the Appendix). Four different cases were simulated for P2D-N assuming a constant biofilm thickness distribution (P2D-N(a) and (b) – Morgenroth *et al.*, 2000a) or using dynamic detachment events (P2D-N(c) and (d) – Morgenroth and Wilderer, 2000). For P2D-N(a) it was assumed that the bulk phase below the maximum biofilm thickness was stagnant (Figure 1A) while for the other three cases the external boundary layer was neglected.

Results

Standard situation (Case 1)

Results for the standard case are shown in Table 6. Using the substrate flux and the effluent substrate concentrations as a performance indicator, all models assuming a flat biofilm yielded virtually identical results. The models differ in the detail of information provided as model outputs. Models 1D-A and 1D-PA do not provide information on the substrate concentration profiles inside the biofilm and do not allow calculation of the substrate concentration at the base of the biofilm. By comparing substrate and oxygen concentrations at the

Table 5 Summary of model definition and assumptions

Model	Descriptions
Flat biofilm morphology	
1D-A Analytical solution	Combination of first order and half-order solution depending on concentration range. Modeler needs to make decision on how to combine first and half-order solutions and averaged based on the Monod term (C_S/K_S+C_S).
1D-PA Pseudo-analytical solution using a spreadsheet	The pseudo-analytical solution takes into account Monod kinetics for the limiting substrate (Saez and Rittmann, 1992).
1D-N Numerical solution of a 1-D biofilm	Different numerical solution procedures were used to describe this 1-D biofilm using (a) standard software (AQUASIM, Wanner and Reichert, 1996), (b) 2-D biofilm simulations (Pizarro <i>et al.</i> , 2001), or (c) 3-D biofilm simulations (Eberl <i>et al.</i> , 2000). Even though 2-D and 3-D numerical solutions were calculated these were for a flat biofilm surface and therefore essentially in the 1-D domain.
Heterogeneous biofilm morphology	
3D-N Numerical solution of a 3-D biofilm	Based on Picioreanu <i>et al.</i> (1998) 3D-N(a): Assumption of a boundary layer parallel to the substratum as shown in Figure 1A. 3D-N(a): Assumption of complete mixing in the pore space of the biofilm with concentrations at the entire surface of the biofilm equal to the bulk phase concentration as shown in Figure 1B.
P2D-N Numerical solution of a pseudo multidimensional biofilm based on the combination of multiple 1-D simulations using AQUASIM	Combination of 1-D simulations to represent a distribution of biofilm thicknesses (Morgenroth and Wilderer, 2000; Morgenroth <i>et al.</i> , 2000a). P2D-N(a): Biofilm thickness distribution with an average thickness of 500 μm and an equal distribution ranging from 50 to 950 μm resulting in 19 separate simulations with an external boundary layer parallel to the substratum as shown in Figure 1A. P2D-N(b): Biofilm thickness distribution with an average thickness of 500 μm and an equal distribution ranging from 50 to 950 μm . No external boundary layer. P2D-N(c): Dynamic detach every 2.3 days with an average biofilm thickness of 500 μm and a base biofilm thickness after detachment of 350 μm . P2D-N(d): Dynamic detach every 7.4 days with an average thickness of 500 μm and a base biofilm thickness after detachment of 10 μm .

base of the biofilm (Models 1D-N) it can be seen that the modeled biofilm is a deep biofilm and that the organic substrate was the limiting factor. Oxygen fully penetrates the biofilm with concentrations $> 9 \text{ mg}_{\text{O}_2}/\text{l}$ at the base of the biofilm while substrate concentrations at the base of the biofilm are very low. The models 1D-A, 1D-PA, and the 1D-N approach based on Pizarro *et al.* (2001) did not allow calculation of the biofilm with multiple soluble components. Thus, these models required the user to decide *a priori* whether oxygen or organic substrate were limiting. In these models, flux and effluent concentration of the

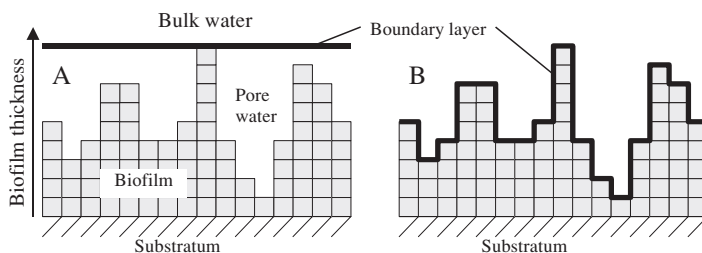


Figure 1 External mass transfer in heterogeneous biofilm systems can be evaluated using the two extreme cases: (A) Mass transport in the pore water is by diffusion only; (B) The pore water and the bulk water are completely mixed

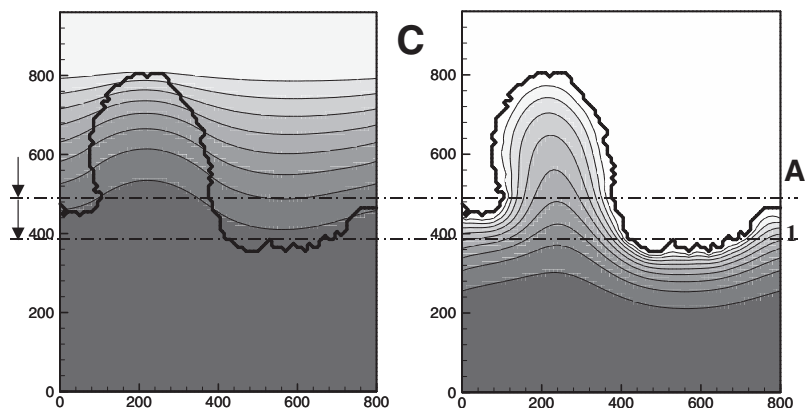


Figure 2 Concentration distribution of COD for the 3D-N(a) (left) and 3D-N(b) (right). Iso-concentration patches for 10% difference in concentration from white (maximum, 12 g/m^3 – left – and 2.3 g/m^3 – right) to dark gray (minimum)

non-limiting component are calculated using stoichiometry linking substrate and oxygen utilization.

In this benchmark study, two basic approaches to model biofilm heterogeneity were tested. The first approach is based on a true 3-D simulation of a heterogeneous biofilm (3D-N(a, b)) while the second approach is based on a combination of results from 1-D simulations (P2D-N(a–d)). The 3-D model 3D-N(b) is a heterogeneous biofilm assuming that substrate concentrations in the pore space are identical to bulk phase concentrations. In that case the increased roughness resulted in an enlargement of the biofilm surface resulting in a 6% increase of the flux into the biofilm compared to flat biofilm simulations. Neglecting any external mass transfer, model P2D-N(b) evaluated the influence of a static biofilm thickness distribution while P2D-N(c) and P2D-N(d) evaluated the influence of local variations of biofilm thickness as a result of dynamic local detachment. Using flux and effluent substrate concentrations as the performance indicator, the variation of biofilm thicknesses ranging from 10 to $950 \mu\text{m}$ for these models did not have a significant influence on overall performance. The overall flux compares well with flat biofilm simulations (Table 6). For the static biofilm thickness distribution ranging from 50 to $950 \mu\text{m}$ (P2D-N(b)) there is a slight increase of the effluent substrate concentrations compared to 1D-N. Dynamic detachment every 2.3 days did not result in any fluctuations of substrate flux because the minimum biofilm thickness after detachment was always larger than the penetration of substrate into the biofilm. For longer detachment intervals (7.4 days) the substrate flux decreased briefly after a detachment event. For the overall performance of the biofilm system both static and dynamic variations of the biofilm thickness yielded similar results. The effect of an enlarged surface area will depend on the penetration depth of the limiting substrate compared to the size of biofilm heterogeneities as will be further discussed in Cases 2 and 3.

The influence of an external mass transport in pores of the heterogeneous biofilm is evaluated in 3D-N(a) and P2D-N(a). In Figure 2, the concentration distribution is compared for 3D-N(a) and 3D-N(b). With the assumption that transport in the pores is due to diffusion only and a concentration boundary layer parallel to the substratum (3D-N(a)) the iso-concentration lines are more or less parallel to the substratum resulting in low concentrations at the biofilm surface in the valleys. For model 3D-N(a) this results in a significant external mass transfer resistance in valleys of the biofilm and the average flux into the biofilm is 30% compared to simulations assuming a flat biofilm. In P2D-N(a) the effect of

Table 6 Summary of key output parameters for the standard case (Case 1). Modeling results in boldface are significantly different and are discussed in the text

		1D-A	1D-PA	1D-N*	3D-N(a)	3D-N(b)	P2D-N(a)	P2D-N(b)	P2D-N(c)	P2D-N(d)
$C_{S,bulk}$	g_{COD}/m^3	4.6	4.4	4.4	12	2.9	12.1	4.6	4.4	4.8
$C_{S,surface}$	g_{COD}/m^3	4.6	4.4	4.4	0.7	2.9	3.2	4.6	4.4	4.8
$C_{S,base}$	g_{COD}/m^3			0.008	0.0037	0.012	0.13	0.48	0.013	0.66
$C_{O_2,bulk}$	g_{O_2}/m^3	10	10	10	10	10	10	10	10	10
$C_{O_2,surface}$	g_{O_2}/m^3	10	10	10	8.1	10	8.3	10	10	10
$C_{O_2,base}$	g_{O_2}/m^3			9.4	7.9	9.5	7.8	9.2	9.2	9.2
$J_{S,surface}$	$g_{COD}/m^2/d$	5.1	5.1	5.1	3.5	5.4	3.6	5.1	5.1	5.0
$J_{O_2,surface}$	$g_{O_2}/m^2/d$	1.9	1.9	1.9	1.3	2	1.3	1.9	1.9	1.9
$L_{F,min}$	μm	500	500	500	340	340	50	50	350	10
$L_{F,max}$	μm	500	500	500	840	840	950	950	618	813
$L_{F,mean}$	μm	500	500	500	500	500	500	500	497	522

* Model predictions from all 1D-N simulations were identical

an increased external mass transfer resistance for lower local biofilm thicknesses was simulated resulting in very similar results compared to 3D-N(a). Overall it can be concluded from the standard case that the different modeling approaches for flat biofilm morphologies had only a minor influence on model predictions while different assumptions for external mass transfers for rough biofilm surfaces had a major influence on predicted substrate flux.

O₂ limitation (Case 2)

Low bulk phase oxygen concentrations resulted in a shift of the limiting component from organic substrate to oxygen as can be seen from the concentrations at the base of the biofilm (Table 7). Oxygen concentrations at the base of the biofilm are virtually zero while substrate is fully penetrating the biofilm. The models 1D-A, 1D-PA, and the 1D-N approach based on Pizarro *et al.* (2001) require the user to decide *a priori* on what the limiting component is for a specific situation. If the non-limiting substrate is in the range of the Monod half-saturation constants there can be a significant influence also of the non-limiting substrate on the overall performance (Qi and Morgenroth, 2003). For simple substrate degradation (as is used in this benchmark study) this decision on the limiting substrate can be made based on ratios of diffusion coefficients and stoichiometric parameters (for details see chapter 5.4 in Henze *et al.*, 2002). Modeling results for all models assuming a flat biofilm surface are similar (except for the approach based on Pizarro *et al.*, 2001) and fluxes into the biofilm are reduced by approximately 56% compared to fluxes in the standard case.

For biofilms with a heterogeneous biofilm surface and an external mass transport resist-

Table 7 Summary of key output parameters for O₂ limitation (Case 2). Modeling results in boldface are significantly different and are discussed in the text. The bulk phase oxygen concentration (*italic*) is according to model definitions (Table 4) and is not calculated by the models

		1D-A	1D-PA	1D-N*	Pizarro <i>et al.</i> (2001)*	3D-N(a)	3D-N(b)
$C_{S,bulk}$	g_{COD}/m^3	19	19	19	20	28	13
$C_{S,base}$	g_{COD}/m^3			18	20	26	12
$C_{O_2,bulk}$	g_{O_2}/m^3	<i>0.20</i>	<i>0.20</i>	<i>0.2</i>	<i>0.20</i>	<i>0.20</i>	<i>0.20</i>
$C_{O_2,base}$	g_{O_2}/m^3			0	0	0	0
$J_{S,surface}$	$g_{COD}/m^2/d$	2.3	2.3	2.2	2	0.41	3.4
$J_{O_2,surface}$	$g_{O_2}/m^2/d$	0.85	0.84	0.81	0.74	0.15	1.3
$J_S: Case2/Case 1$	%	45	45	43	39	12	63
$L_{F,mean}$	μm	360	359	350	500	350	350

* Model predictions following the approach of Pizarro *et al.* (2001) were significantly different from other simulations in 1D-N and are shown separately for this case

ance in the pore space (3D-N(a)) the reduced oxygen concentration in the bulk phase reduces the fluxes by 88% compared to fluxes in the standard case. With lower bulk phase concentrations the effect of the external mass transfer resistance is becoming more and more significant. For the present case of low oxygen concentrations, the penetration depth of oxygen is small compared to the biofilm structure. Thus, for 3D-N(b) the low bulk phase oxygen concentration results in the reduction of fluxes only by 37% compared to the standard case fluxes. Overall it can be concluded that biofilm morphology and the external mass transfer resistance in the pore space have a significant influence on modeling results.

Biomass limitation (Case 3)

For the case of biomass limitation, all models (except for the approach based on Pizarro *et al.*, 2001, due to the coarse discretization) resulted in similar model predictions independent of biofilm morphology (Table 8). These modeling results illustrate well that external mass transfer and internal mass transport do not influence overall substrate degradation if the total amount of biomass is limiting. As can be seen from the concentrations at the base of the biofilm, the biofilm was fully penetrated and neither transport of oxygen nor of organic substrate was limiting.

Reduced diffusivity in the biofilm (Case 4)

A reduction of the diffusion coefficient inside the biofilm by 80% resulted in the reduction of the fluxes into the biofilm by approximately 20% for models assuming a flat biofilm (Table 9). This rather limited influence of the diffusion coefficient on model predictions can be explained by considering half order biofilm kinetics (Harremoës, 1976). According to half order kinetics the overall substrate flux is proportional to $\sqrt{D_f}$ and to $\sqrt{C_S}$. For a given bulk phase concentration, a decrease of the diffusion coefficient by a factor of 5 results in a decreased flux into the biofilm by a factor of 2.2. Based on the mass balance for the overall

Table 8 Summary of key output parameters for biomass limitation (Case 3). Modeling results in boldface are significantly different and are discussed in the text

		1D-A	1D-PA	1D-N*	Pizarro <i>et al.</i> (2001)*	3D-N(a)
$C_{S,bulk}$	g_{COD}/m^3	21	22	22.0	17.2	22
$C_{S,base}$	g_{COD}/m^3			22.0	16.9	22
$C_{O_2,bulk}$	g_{O_2}/m^3	10	10	10	10	10
$C_{O_2,base}$	g_{O_2}/m^3			10	10	9.9
$J_{S,surface}$	$g_{COD}/m^2/d$	1.9	1.6	1.6	2.6	1.6
$J_{O_2,surface}$	$g_{O_2}/m^2/d$	0.7	0.58	0.6	0.96	0.59
J_S : Case 3/Case 1	%	37	31	31.2	51	46
$L_{F,mean}$	μm	20	20	20	20	19

* Model predictions following the approach of Pizarro *et al.* (2001) were significantly different from other simulations in 1D-N and are shown separately for this case

Table 9 Summary of key output parameters for increased internal diffusion resistance (Case 4). Modeling results in boldface are significantly different and are discussed in the text

		1D-A	1D-PA	1D-N	3D-N(a)	3D-N(b)
$C_{S,bulk}$	g_{COD}/m^3	9.2	9.4	9.6	22	6.1
$C_{S,base}$	g_{COD}/m^3			0	0.42	0
$C_{O_2,bulk}$	g_{O_2}/m^3	10	10	10	10	10
$C_{O_2,base}$	g_{O_2}/m^3			8.8	0	4.9
$J_{S,surface}$	$g_{COD}/m^2/d$	4.2	4.1	4.0	1.8	4.8
$J_{O_2,surface}$	$g_{O_2}/m^2/d$	1.5	1.5	1.5	0.56	1.8
J_S : Case 4/Case 1	%	82	80	79	51	89
$L_{F,mean}$	μm	500	500	500	500	500

Table 10 Summary of key output parameters for an external boundary layer (Case 5). Modeling results in boldface are significantly different and are discussed in the text

		1D-A	1D-PA	1D-N	3D-N(a)	3D-N(b)
$C_{S,bulk}$	g_{COD}/m^3	16	16	15.7	19	16
$C_{S,surface}$	g_{COD}/m^3	2.5	2.1	2.2	7.5	1.4
$C_{S,base}$	g_{COD}/m^3			0.0092	0.005	0.005
$C_{O_2,bulk}$	g_{O_2}/m^3	10	10	10	10	10
$C_{O_2,surface}$	g_{O_2}/m^3		7.4	8.3	7.9	7.4
$C_{O_2,base}$	g_{O_2}/m^3			8.1	5.9	7.1
$J_{S,surface}$	$g_{COD}/m^2/d$	2.8	2.8	2.8	2.3	2.9
$J_{O_2,surface}$	$g_{O_2}/m^2/d$	1	1	1.1	0.83	1.1
$J_S: Case 5/Case 1$	%	55	55	56	66	54
$L_{F,mean}$	μm	430	439	467	495	495

reactor a decreased flux will increase the bulk phase substrate concentration, which increases the substrate flux. Overall, the significant decrease of the diffusion coefficient ends up having only a minor influence on the overall flux. For model 3D-N(a), the decreased diffusion coefficient results in an increase in external mass transfer resistance within the pores resulting in a significant decrease of the flux compared to case 1 (reduction by 44%). Model 3D-N(b) has an enlarged surface area, which becomes more and more of an advantage as mass transport inside the biofilm becomes limiting. Thus, for model 3D-N(b) the flux into the biofilm decreases only by 11% compared to the 20% reduction of the flat biofilm models.

Mass transfer resistance in the bulk (Case 5)

For the case of an increased external mass transfer resistance, simulations assuming a flat biofilm and 3D-N(b) resulted in very similar fluxes (Table 10). For model 3D-N(a) the relative flux reduction compared to the standard case is only 34% compared to an approximate 45% reduction for the other models. As 3D-N(a) assumes an external mass transfer resistance in the pore space for all simulations, the effect of an increased external mass transfer resistance has a smaller impact compared to other models neglecting any external mass transfer resistance for all other cases.

Conclusion

In this benchmark (BM1) a biofilm system was defined and evaluated for five cases where overall conversion for different cases was limited by the amount of biomass, by internal mass transport, or by external mass transfer. The benchmark was used to compare different modeling approaches ranging from analytical models to multi dimensional models requiring the use of high performance computing. It was shown that modeling results were not significantly different for all modeling approaches assuming a flat biofilm morphology. Assuming a heterogeneous biofilm morphology modeling results were mainly influenced by the assumption on mass transfer in the pores within the biofilm. If mass transfer within the pore volume was by diffusion then overall fluxes decreased significantly. With the assumption of concentrations within the pore volume being equal to bulk phase concentrations then the enlarged surface area resulted in a slight increase of fluxes into the biofilm. While modeling results were very similar for the different modeling approaches the efforts involved in solving these models were not. Multi-dimensional models required modifications of custom made software and in some cases extensive computing power. Thus, for simple and more or less smooth biofilms systems, the use of analytical, pseudo-analytical or simple numerical 1-D models is a good compromise between required modeling output and effort involved in solving these models.

Acknowledgements

This material is based in part upon work supported by a CAREER award to Eberhard Morgenroth from the National Science Foundation under grant No. BES-0134104.

References

- Eberl, H.J., Picioreanu, C., Heijnen, J.J. and van Loosdrecht, M.C.M. (2000). A three-dimensional numerical study on the correlation of spatial structure, hydrodynamic conditions, and mass transfer and conversion in biofilms. *Chem. Eng. Sci.*, **55**(24), 6209–6222.
- Eberl, H.J., van Loosdrecht, M.C.M., Morgenroth, E., Noguera, D.R., Picioreanu, C., Perez, J., Rittmann, B.E., Schwarz, A.O. and Wanner, O. (2004). Modelling a spatially heterogeneous biofilm and the bulk fluid: selected results from Benchmark Problem (BM2). *Wat. Sci. Tech.* **49**(11–12), 155–162 (following article).
- Harremoës, P. (1976). The significance of pore diffusion to filter denitrification. *J. Water Pollut. Control Fed.*, **48**(2), 377–388.
- Henze, M., Harremoës, P., Jansen, J. la C. and Arvin, E. (2002). *Wastewater Treatment*. 3 Springer, Berlin. ISBN: 3540422285.
- Morgenroth, E. and Wilderer, P.A. (2000). Influence of detachment mechanisms on competition in biofilms. *Wat. Res.*, **34**(2), 417–426.
- Morgenroth, E., Eberl, H.J. and van Loosdrecht, M.C.M. (2000a). Evaluating 3-D and 1-D mathematical models for mass transport in heterogeneous biofilms. *Wat. Sci. Tech.*, **41**(4–5), 347–356.
- Morgenroth, E., van Loosdrecht, M.C.M. and Wanner, O. (2000b). Biofilm models for the practitioner. *Wat. Sci. Tech.*, **41**(4–5), 509–512.
- Noguera, D.R. and Morgenroth, E. (2004). Introduction to the IWA Task Group on Biofilm Modeling. *Wat. Sci. Tech.* **49**(11–12), 131–136 (this issue).
- Picioreanu, C., van Loosdrecht, M.C.M. and Heijnen, J.J. (1998). Mathematical modeling of biofilm structure with a hybrid differential discrete cellular automaton approach. *Biotech. Bioengr.*, **58**(1), 101–116.
- Pizarro, G., Griffeath, D. and Noguera, D.R. (2001). Quantitative cellular automaton model for biofilms. *J. Environ. Eng.-ASCE*, **127**(9), 782–789.
- Qi, S.Y. and Morgenroth, E. (2003). Modeling Steady-State Biofilms with Dual-Substrate Limitations. *Accepted for publication in ASCE J. of Environmental Engineering*.
- Rittmann, B.E., Schwarz, A.O., Eberl, H.J., Morgenroth, E., Perez, J., van Loosdrecht, M.C.M. and Wanner, O. (2004). Results from the multi-species Benchmark Problem (BM3) using one-dimensional models. *Wat. Sci. Tech.* **49**(11–12), 163–168 (this issue).
- Saez, P.B. and Rittmann, B.E. (1992). Accurate pseudoanalytical solution for steady state biofilms. *Biotech. Bioengr.*, **39**(7), 790–793.
- Wanner, O. and Reichert, P. (1996). Mathematical-modeling of mixed-culture biofilms. *Biotech. Bioengr.*, **49**(2), 172–184.
- Wanner, O. and Morgenroth, E. (2004). Biofilm modeling with AQUASIM. *Wat. Sci. Tech.* **49**(11–12), 137–144.